Int. J. Electrochem. Sci., 11 **(2016)** 4771 – 4778, doi: 10.20964/2016.06.67

International Journal of
ELECTROCHEMICAL
SCIENCE
www.electrochemsci.org

Short Communication

Effect of Temperature on Electrochemical Performance of $LiMg_{0.06}Mn_{1.94}O_4$ Prepared by a Molten-Salt Combustion Method

Junming Guo[1,2,3,*], *Lei Hu*[1,2,3], *Chang-wei Su*[1,2,3], *Rui Wang*[1,2,3], *Xiaofang Liu*[1,2,3], *Jinhui Peng*[1,2,3*]

[1] Key Laboratory of Comprehensive Utilization of Mineral Resources in Ethnic Regions, Yunnan Minzu University, Kunming 650500, *PR* China
[2] Key Laboratory of Resource Clean Conversion in Ethnic Regions, Education Department of Yunnan, Yunnan Minzu University, Kunming 650500, *PR* China
[3] Joint Research Centre for International Cross-border Ethnic Regions Biomass Clean Utilization in Yunnan, Yunnan Minzu University, Kunming 650500, PR China
[*]E-mail: guojunming@tsinghua.org.cn

Received: 14 February 2016 / *Accepted:* 28 March 2016 / *Published:* 4 May 2016

$LiMg_{0.06}Mn_{1.94}O_4$ cathode materials were synthesized by a molten-salt combustion method at 400 ℃ for 1h and two- step calcination at 500 °C, 600 °C, 700 °C and 800 °C for 3h. The temperature effect on the crystal structure and the morphology of $LiMg_{0.06}Mn_{1.94}O_4$ has been evaluated by X-ray diffraction (XRD) analysis and scanning electron microscopy (SEM). The materials synthesized at 600 °C and 700°C were single phase, while Mn_2O_3 and Mn_3O_4 impurity phases can be detected in the other materials synthesized at 800 °C and 900 °C, respectively. The average particle size of $LiMg_{0.06}Mn_{1.94}O_4$ increased with the increase of calcination temperature. The effect of the calcination temperature on the electrochemical performances of the $LiMg_{0.06}Mn_{1.94}O_4$ materials has also been studied by galvanostatic charge/discharge tests and cyclicvoltammetry (CV) measurements. The results showed that the prepared $LiMg_{0.06}Mn_{1.94}O_4$ at 600 °C and 700°C demonstrated better electrochemical performance than the ones at 500 °C and 800°C, with an initial discharge specific capacity of 117.7 mAh g^{-1} and 112.8 mAh g^{-1}, and their capacity retention was 78.2% and 79.3% after 100 cycles at 0.5 C, respectively.

Keywords: Lithium-ion battery; $LiMg_{0.06}Mn_{1.94}O_4$; cathode materials; Electrochemical performance; molten-salt combustion method

1. INTRODUCTION

Nowadays, lithium-ion batteries (LIBs) have been widely used for the power sources in the myriad portable electric devices due to their excellent electrochemical performance [1, 2]. The safety

concerns of LIBs seem to be the more seriously cared [3]. Due to its high safety, spinel $LiMn_2O_4$, as a positive-electrode material with 3D tunnel structure for the transportation of Li^+ ions, has received a great deal of attention [4-7].

Unfortunately, the use of spinel $LiMn_2O_4$ as the cathode of LIBs is precluded by its capacity fading. This capacity fading is suggested to be the main result from the structural distortion of spinel $LiMn_2O_4$ via the replace of Mn^{2+} by the Jahn-Teller active Mn^{3+} ion [8-10]. Thus, substitutions of the Jahn-Teller active Mn^{3+} ions by other cations (e.g. Li, Al, Mg, Co, Cr, Cu, Ni), have been thought to be an effective way for the suppression of capacity fading for spinel $LiMn_2O_4$ [11-17]. Magnesium a preferred dopant for $LiMn_2O_4$ since it is abundant, eco-friendly, low-cost, less expensive and lighter than transition metal elements. Mg-doping $LiMn_2O_4$ has shown the distinct improvement of capacity fading by improving the structural stability, which is attributed to increasing relative amount of Jahn-Teller inactive Mn^{4+} ion [14, 18-20]. Generally, cation-substituted spinel $LiMn_2O_4$ was mainly prepared by solid-state method [21], sol-gel method [12], molten salts synthesis [22], co-precipitation method [23], solid-state combustion synthesis [14], molten-salt combustion methods [20] and so on. Among these methods, the molten-salt method generally uses carbonate or hydroxide as a raw material and excess KCl or LiOH as a molten medium or reactant. After preparation, the samples need to be washed with ethanol or distilled water to remove the excess KCl or Li salt, which makes the process more complex [22]. The molten-salt combustion methods to produce ion-doped $LiMn_2O_4$ are attractive because of their rapid reaction rate, simplicity and low cost; in addition, stoichiometric products can be obtained. Huang et al [20] prepared spinel $LiMg_xMn_{2-x}O_4$ ($x \leq 0.10$) by a molten-salt combustion method and showed that Mg-doped samples can improve the cyclic performance and rate capacity compared to the $LiMn_2O_4$. However, there are few reports where Mg-doped LiMn2O4 is obtained using the molten-salt combustion method at various heat treatment temperatures.

In this work, the molten-salt combustion method was utilized to prepare the $LiMg_{0.06}Mn_{1.94}O_4$ cathode materials using acetate raw materials. This method does not need the addition of other fuel, and raw materials realize self-mixing by heating directly. The influence of calcinations temperature on the crystal structure, morphology, and electrochemical properties of the $LiMg_{0.06}Mn_{1.94}O_4$ cathode materials was also investigated.

2. EXPERIMENTAL

2.1. Preparation of samples

Spinel $LiMg_{0.06}Mn_{1.94}O_4$ samples were synthesized by a molten-salt combustion method. Stoichiometric amounts of lithium acetate (AR, alading), manganese acetate (AR, alading) and magnesium acetate (AR, alading) were weighed, and blended in a 300 mL porcelain crucible. After preheating at 400 °C for 1h in a muffle furnace, the mixture was ground and sintered at calcination temperatures for 3h, followed by cooling down to room temperature to obtain the final product $LiMg_{0.06}Mn_{1.94}O_4$ powders. To explore the impact of calcination temperatures on the electrochemical properties of $LiMg_{0.06}Mn_{1.94}O_4$, diverse temperature values of 500 °C, 600 °C, 700 °C and 800 °C were

chosen as the research objects. For convenience, the products prepared at 500℃, 600℃, 700℃and 800℃ are marked as II500, II600, II700 and II800, respectively。

2.2. Characterization

The crystalline structure of samples was characterized by X-ray diffraction (XRD; D/max-TTRIII, Rigaku, Japan) with Cu Kα radiation operated at 30 mA and voltage of 40 kV in the 2θ angular range of 10-70° at 4° min^{-1} with 0.02° step size. Lattice parameters were obtained by Jade 5.0 software. The morphology of the $LiMg_{0.06}Mn_{1.94}O_4$ powders was detected by scanning electron microscopy (SEM; Quanta-200, FEI, Hillsboro, OR, USA).

2.3. Electrochemical measurements

The mixture, which is composed of 80 wt.% active powder $LiMg_{0.06}Mn_{1.94}O_4$, 10 wt.%, acetylene black 10 wt.% polyvinylidene difluoride, were blended in N-methyl-2-pyrrolidone to form a homogeneous slurry. After pasting onto an Al foil by a doctor-blade technique, the slurry was dried at 120 °C overnight in a vacuum oven to obtain the cathodes. The cathodes were then cut by roll-press. For electrochemical measurements, CR2025 coin-type cells were assembled in an argon-filled glove box using a polypropylene microporous film (Celgard 2320) separator between the prepared cathodes and Li foil anode, 1.0 M $LiPF_6$ dissolved in ethylene carbonate and dimethyl carbonate (1:1 in volume) as the electrolyte. The cells of galvanostatic charge and discharge were tested by a Land electric test system (CT2000A, Wuhan Jinnuo Electronics Co., Ltd., China) in the potential range between 3.0 and 4.5 V at 0.5 C. Cyclic voltammetry (CV) was performed on an electrochemical workstation (IM6ex, Zahner Elektrik GmbH&Co. KG, Germany) at a scanning rate of 0.05 mV s^{-1} in the voltage range of 3.5-4.6 V. Electrochemical impedance spectroscopy (EIS) was recorded on the same electrochemical workstation with the frequency range from 0.1 Hz to 100 KHz and an 10mV AC signal amplitude .

3. RESULTS AND DISCUSSION

3.1 X-ray diffraction analysis

Fig.1 shows the XRD patterns of $LiMg_{0.06}Mn_{1.94}O_4$ powders prepared by the molten-salt combustion method. The XRD patterns of all samples presented in Fig. 1 exhibit all the diffraction peaks corresponding to the cubic spinel $LiMn_2O_4$ with the Fd3m space group (JCPDS, PDF35-0782)[24], suggested that the spinel structure of $LiMn_2O_4$ could be synthesised by the two-step calcinations process. The crystallinity of synthesized materials increased with the increase of calcination temperature. The materials synthesized at II600 and II700 were single phase. The impurity was Mn_2O_3 at II500 materials, while at II800 materials, the impurity phase abruptly transformed into Mn_3O_4 which could be attributed to that the II800 sample demonstrated more decomposition so that generated more Mn_3O_4 impurities at a higher temperature. The lattice parameters of the materials are

summarized in Table 1. The results showed that the lattice parameters grow up with the extension of calcinations temperature, which indicates that the enhancement of calcination temperature was beneficial for the expansion of unit cell. In addition, the lattice parameters of all materials were less than the standard value (8.247Å) of spinel $LiMn_2O_4$, because of Mn^{3+} (0.645 Å) ions are replaced by Mg^{2+} (0.650 Å) ions, as well as Mn^{3+} (0.645 Å) ions translated to Mn^{4+} (0.53 Å) ions, which indicated that Mg^{2+} ions were doped into the spinel $LiMn_2O_4$ lattice [25].

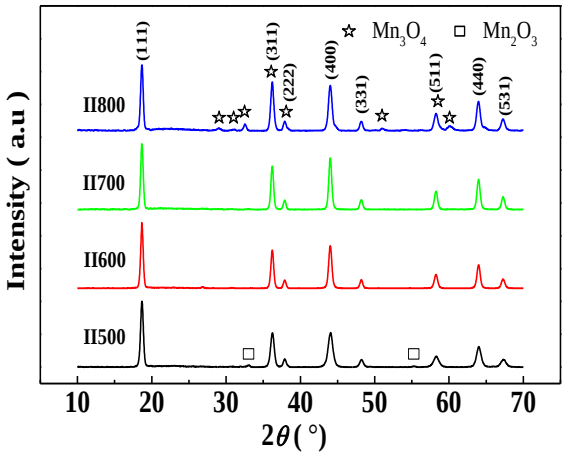

Figure 1. XRD patterns of $LiMg_{0.06}Mn_{1.94}O_4$ materials prepared at different calcination temperatures.

Table 1. Lattice parameter of the prepared $LiMg_{0.06}Mn_{1.94}O_4$ samples

Samples	Lattice parameters (Å)
II500	8.2231
II600	8.2295
II700	8.2299
II800	8.2308

3.2 Morphology and particle size analysis

The SEM images of $LiMg_{0.06}Mn_{1.94}O_4$ powders are presented in Fig. 2 prepared at 400 °C for 1 h and two-stage calcination at 500 °C, 600 °C, 700 °C and 800 °C for 3h. All materials exhibited an inhomogeneous distribution. The materials calcined at lower temperature showed agglomeration. It can be observed from Fig. 2 that the average particle size of II500 and II600 materials was not significantly changed, while that of II700 and II800 materials were increased from about 0.5 μm to 1.0 μm, implying that the grains grow more completely, larger particle size and weaker agglomeration, with the increase of calcination temperature. At the calcination temperature from 700 °C to 800 °C, the grains had a spinel-like structure with clear edges. At the high-temperature calcinations of 800 ℃, the grains revealed much clearer particle interface.

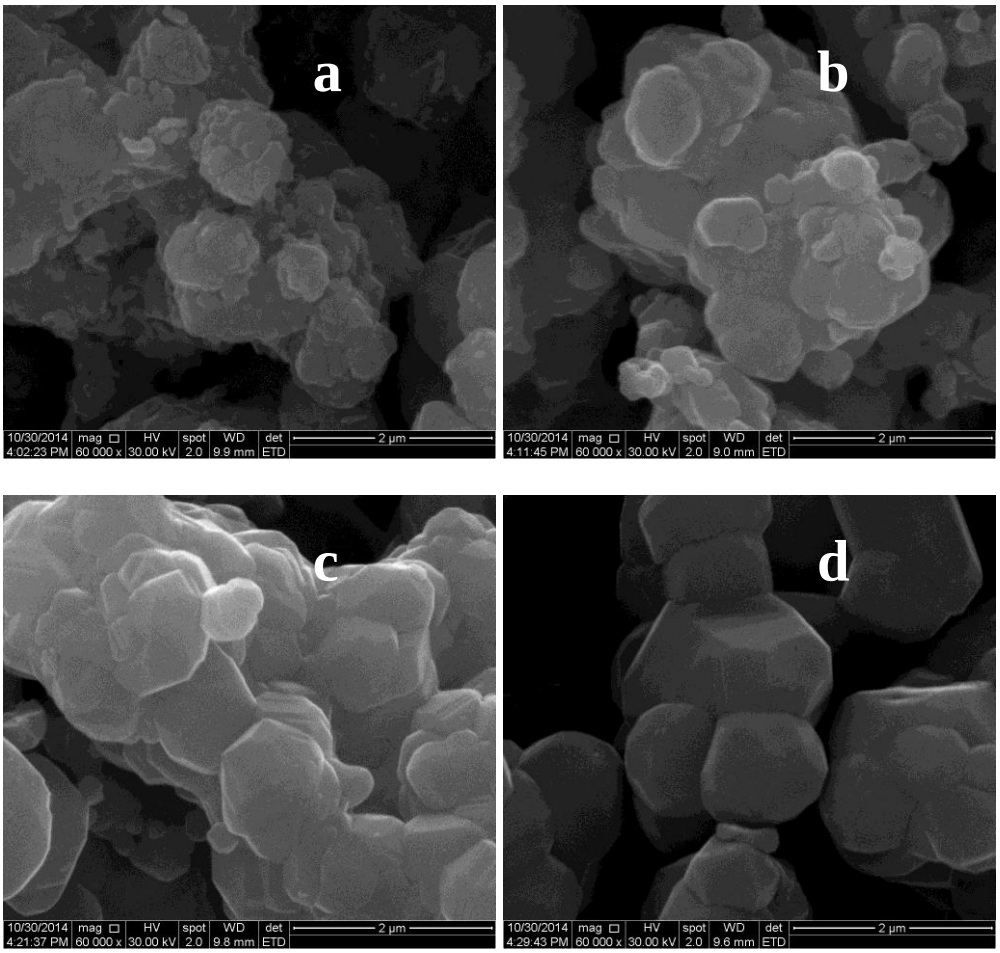

Figure2. SEM images of the $LiMg_{0.06}Mn_{1.94}O_4$ materials prepared at different calcinations temperatures: II500 (a), II600 (b), II700 (c), and II800 (d).

3.3 Galvanostatic charge/discharge behavior

Fig. 3(a) and (b) display the initial galvanostatic discharge profiles and cycling performance curves of all the $LiMg_{0.06}Mn_{1.94}O_4$ materials between 3.0 V and 4.5V (vs. Li / Li^+) at 0.5 C. All the samples display two voltage plateaus at 3.9-4.2 V, corresponding to Li^+ insertion/extraction at two different tetragonal 8a sites in the spinel framework [26].Fig. 3 and Table 2 show the discharge specific capacities of all products were 82.6, 92.1, 89.5 and 54.9 mAh g^{-1} and the capacity retentions were 81.1%, 78.2%, 79.3% and 68.8% after 100 cycles, respectively. The sample of II500 shows the highest capacity retention, with a lower initial discharge specific capacity. Compared with the sample of II600, which was higher than those of the other samples. Hence, the II600 product shows a better electrochemical performance.

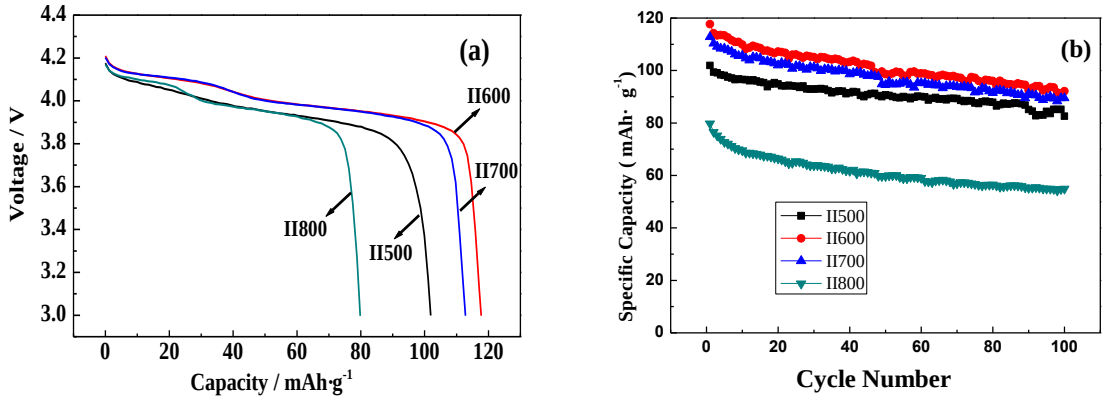

Figure 3. Potential profiles and first cycle discharge capacity of the products at the current densities of 0.5 C (a), and cycle performances at current of 0.5 C (b).

Table 2. Initial, 100th discharge capacities, and capacity retention of the prepared $LiMg_{0.06}Mn_{1.94}O_4$ samples

Cathode material	1st discharge capacity (mAh/g)	100th discharge capacity (mAh/g)	Capacity retention (%)
II500	101.9	82.6	81.1
II600	117.7	92.1	78.2
II700	112.8	89.5	79.3
II800	79.8	54.9	68.8

3.4. Electrochemical behavior

The typical cyclic voltammograms of II500 and II600 after the completion of 100th cycles at a scan rate of 0.05 mVs^{-1} in the potential range between 3.60 and 4.50 V. Fig. 4 shows that the II600 sample exhibited higher peak current and peak area, indicating higher discharge specific capacity and electrochemical activity.

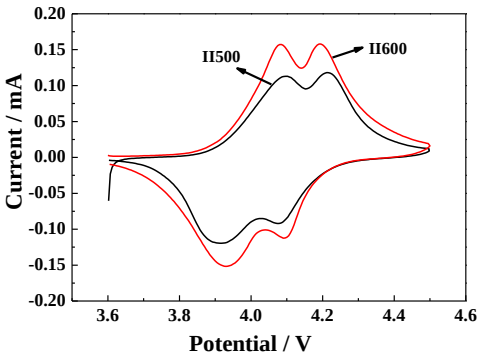

Figure 4. CV curves of II500 and II600 in the voltage range of 3.60 – 4.50 V (0.05 mV/s).

For the II500, both anodic and cathodic peaks are broader and closed to each other with weaker intensity of peaks current compared to II600, indicating II600 has smaller polarization and better reversibility[15,27]. Based on the results, II600 has better reversibility and electrochemical performances.

4. CONCLUSIONS

The spinel $LiMg_{0.06}Mn_{1.94}O_4$ cathode materials were successfully synthesized by the molten-salt combustion method at different calcination temperatures (500 °C, 600 °C, 700 °C and 800 °C). XRD characterization exhibited that II600 and II700 materials are single phase, while Mn_2O_3 and Mn_3O_4 impurity phases can be detected in the other materials synthesized at 800 °C and 900 °C, respectively. The particle size of $LiMg_{0.06}Mn_{1.94}O_4$ materials increased with the increase of calcinations temperature. Moreover, the II600 and II700 materials revealed excellent electrochemical performance with initial discharge specific capacity of 117.7 and 112.8 mAh g^{-1}, and capacity retention of 78.2% and 79.3% after 100 cycles at 0.5 C, respectively. Thus, the calcinations temperature is an important parameter for the preparation of $LiMg_{0.06}Mn_{1.94}O_4$ materials by molten-salt combustion method using the acetate raw material.

ACKNOWLEDGEMENTS
This work was financially supported by the National Natural Science Foundation of China (51262031, 51462036), Program for Innovative Research Team (in Science and Technology) in University of Yunnan Province (2011UY09), Yunnan Provincial Innovation Team (2011HC008).

References

1. J.M. Tarascon and M. Armand, *Nature*, 414(2001) 359-367.
2. M.S. Whittingham, *Chem. Rev.*, 114(2014) 11414-11443.
3. P.G. Balakrishnan, R. Ramesh and T. Prem Kumar, *J. Power Sources*, 155(2006) 401-404.
4. D. Guyomard and J.M. Tarascon, *Solid State Ionics*, 69(1994) 222-237.
5. Y.Y. Xia, H. Takeshige, H. Noguchi and M. Yoshio, *J. Power Sources*, 56(1995) 61-67.
6. W. Liu, G.C. Farrington, F. Chaput and B. Dunn, *J. Electrochem. Soc.*, 143(1996) 879-884.
7. Y. Gao and J. Dahn, *J. Electrochem. Soc.*, 143(1996) 100-114.
8. H. Gadjov, M. Gorova, V. Kotzeva, G. Avdeev, S. Uzunova and D. Kovacheva, *J. Power Sources*, 134(2004) 110-117.
9. K. Matsuda and I. Taniguchi, *J. Power Sources*, 132(2004) 156-160.
10. R.J. Gummow, A. De Kock and M. Thackeray, *Solid State Ionics*, 69(1994) 59-67.
11. Z.D. Peng, Q.L. Jiang, K. Du, W.G. Wang, G.R. Hu, Y.X. Liu, *J. Alloys Compd.*, 493 (2010)640-644.
12. W.W.Wu·J.J.Chen·S.Cheng·H.F.Xiang, Ionics,21(2015) 1843-849
13. D.L. Fang, J.C. Li, X. Liu, P.F. Huang, T.R. Xu, M.C. Qian and C.H. Zheng, *J. Alloys Compd.*, 640 (2015) 82-89.
14. M.W. Xiang, C.W. Su, L.L. Feng, M.L. Yuan and J.M. Guo, *Electrochim. Acta*, 125 (2014) 524-529.

15. X.Yi, X.Y. Wang, B.W.Ju, Q.Li. Wei, X.K .Yang,G.S. Zou,H.B. Shu,L. Hu, *Journal of Alloys and Compouds*, 604(2014)50-56.
16. J.J. Huang, Q.L. Li, H.L. Bai, W.Q. Xu, Y.H. He, C.W. Su, J.H. Peng and J.M. Guo, *Int. J. Electrochem. Sci.*, 10 (2015) 4596 - 4603.
17. K. Nakura, Y. Ohsugi, M. Imazaki, K. Ariyoshi and T. Ohzuku, *J. Electrochem. Soc.*, 158(2011) A1243-A1249.
18. F.P. Nkosi, C.J. Jafta, M. Kebede, L. le Roux, M.K. Mathe, K. Mkhulu and K.I. Ozoemena, *RSC Advances*, 5(2015)32256-32262.
19. K. Suryakala, G.P. Kalaignan and T. Vasudevan, *Int J Electrochem Sci*, 1(2006) 372.
20. J.J. Huang, F.L. Yang, Y.J. Guo, C.C. Peng, H.L. Bai, J.H. Peng and J.M. Guo, *Ceramics International*, 41(2015)9662–9667.
21. A.B. Yuan, L. Tian, W.M. Xu and Y.Q. Wang, *J. Power Sources*, 195(2010)5032–5038.
22. S.J. Shi, J.P. Tu, Y.Y. Tang, X.Y. Liu, X.Y. Zhao, X.L. Wang and C.D. Gu, *J. Power Sources*, 241 (2013)186-195.
23. R. Thirunakaran, R. Ravikumar, S. Gopukumar and A. Sivashanmugam, *J. Alloys Compd.*, 556(2013)266–273.
24. H.Y. Zhao, X.Q Liu, C. Cheng, Z. Zhang, Y. Wu, B. Chen, W.Q. Xiong, *J Solid State Electrochem.*, 19(2015) 1015-1026.
25. M.W. Xiang, L.Q. Ye, C.C. Peng, L. Zhong, H.L. Bai, C.W. Su and J.M. Guo, *Ceramics International*, 40(2014)10839–10845.
26. W.C. Wen, B.W. Ju, X.Y. Wang, C. Wu, H.B. Shu, X.K. Yang, *Electrochim Acta*, 147(2014)271-278
27. B.S. Qin, Z.H. Liu, G.L. Ding, Y.L. Duan, C.J. Zhang, G.L. Cui, *Electrochim Acta*, 141(2014)162-172